Nanostructured Sn doped WO_3 thin films prepared by electron beam evaporation

R. Ravi Kumar, P. Jabbar Khan, D. Sampurna Rao, A. Sivasankar Reddy*

Department of Physics, Vikrama Simhapuri University, Nellore-524324, Andhra Pradesh, India

***Corresponding Author:**A. Sivasankar Reddy;**Emai: akepati77@gmail.com*

Abstract: In the present work, nanostructured tin doped tungsten oxide (Sn-WO_3) thin films were prepared on glass substrate by electron beam evaporation at different wt% of tin(Sn).Structural, microstructural, chemical and optical properties of the films were systematically studied. The WO_3 films exhibited an amorphous nature, and the amorphous nature of the WO_3 films did not change even after doped with different Sn concentration to WO_3. The microstructure of the WO_3 films changed from nanoflakes to rose flakes structure at 5wt% of Sn doping to WO_3. On further increasing the dopant concentration to 10wt%, the rose flakes turned into nano nails. The bandgap of the films reduced gradually from undoped to Sn doped WO_3films.

Keywords – Thin Films, Electron Beam Evaporation, Nanostructure, Tungsten Oxide

I. INTRODUCTION

Nanostructures consist of particles, ribbon, mesh, rods, sheets, springs, wires, belts,rings, and many more, and these nanostructureshave shown great potential in various applications due to the quantum confinement effect, electrical, optical and mechanical properties, changed density of states, high surface-to-volume ratio, and lowdimensionality. Nanostructured metal oxide thin-films such as ZnO, TiO_2, SnO_2, Fe_2O_3, MoO, NiO, and WO_3 are generally applied as gas sensitive materials and suitable for gas detection due to their unique properties, such as typical surface properties and reproducibility [1-8]. Among these materials, tungsten oxide (WO_3) is one of the best material due its physical,chemical and electrical properties, variety in structural orientations, and it possess variety of applications like sensors, antibacterial coatings, batteries, photoluminescence, photochromic, photocatalysis, electrochromic and smart windows[9-13]. WO_3 based thin films are prepared using several methods, such as electron beam evaporation [14], sputtering [15], resistivity heating [16], spray [17], sol-gel [18], and electrodeposition [19]. In this study, electron beam evaporation was used to prepare a novel type of WO_3 and Sn doped WO_3 nanostructured films and study the physical properties of the films.

II. EXPERIMENTAL

Tungsten oxide (WO_3) and tin-doped tungsten oxide (Sn-WO_3) pellets were used to prepare nanostructured thin films by electron beam evaporation technique onto the glass substrates. WO_3 and Sn-WO_3 pellets were prepared using high purity (99.99%) of WO_3 and Sn powders. The thicknesses of the films were approximately 260 nm. The parameters maintained during the deposition of the films are listed in Table 1.

Table-1 The parameters maintained during the deposition of the films are listed in.

S. No.	Parameters	WO_3 Films	Sn-WO_3 Films		
			5 wt%	10 wt%	15 wt%
1	Accelerating Voltage (kV)	48	48	48	48
2	Accelerating Current (mA)	1.3	1.3	1.3	1.3
3	Base Pressure(mbar)	3.8×10^{-6}	3.8×10^{-6}	3.8×10^{-6}	3.8×10^{-6}
4	Deposition Pressure (mbar)	1×10^{-3}	1×10^{-3}	1×10^{-3}	1×10^{-3}
5	Deposition Time (min)	10	12	12	12
6	Deposition Temperature	Room Temperature	Room Temperature	Room Temperature	Room Temperature

2.1 Characterization of WO_3 and Sn-WO_3 nanostructured films

The structural properties of the films were recorded using an X-ray diffractometer (XRD) and the microstructure was analyzed by scanning electron microscopy (SEM). The chemical composition was studied using energy dispersive spectroscopy (EDS). The optical properties of the films were recorded by UV-Vis-NIR

double beam spectrometry.

III. RESULTS AND DISCUSSION

3.1. Microstructure and compositional analysis

Figure 1 (a-d). shows the SEM images of nanostructured WO_3 and Sn doped WO_3 films. Fig. 2(a) shows that the WO_3 films exhibited a smooth, crack free surface, and homogenous nanoflakes were uniformly distributed on the substrate surface. The microstructure of the films changed when the WO_3 films were doped with 5 wt% of Sn (Fig. 2(b)). The nanoflakes agglomerated together and a formed rose flakes structure. On further increasing the dopant concentration to 10wt%, the rose flakes structure turned into nano nails (Fig. 2(c)).Beyond this dopant concentration, nano nails are disappear and completely differentnanostructure (water fungi type structure) is formedin 15wt% Sn doped WO_3 films (Fig. 2(d)), and this may be due to arising of structural defects in the films. From the SEM results, the Sn doping is significantly changed the microstructure of WO_3 films. At initially,Sn supports the growth of the nanostructure of WO_3, and it continues to until a certain dopant concentration reached.Shankara et al. [20], observed similar microstructural changes in Sn-WO_3 with Sn concentration. After Sn doping to the WO_3, a noticeable change in morphology was observed, due to the substitution of Sn in the crystal lattice, which affects the structure of WO_3.

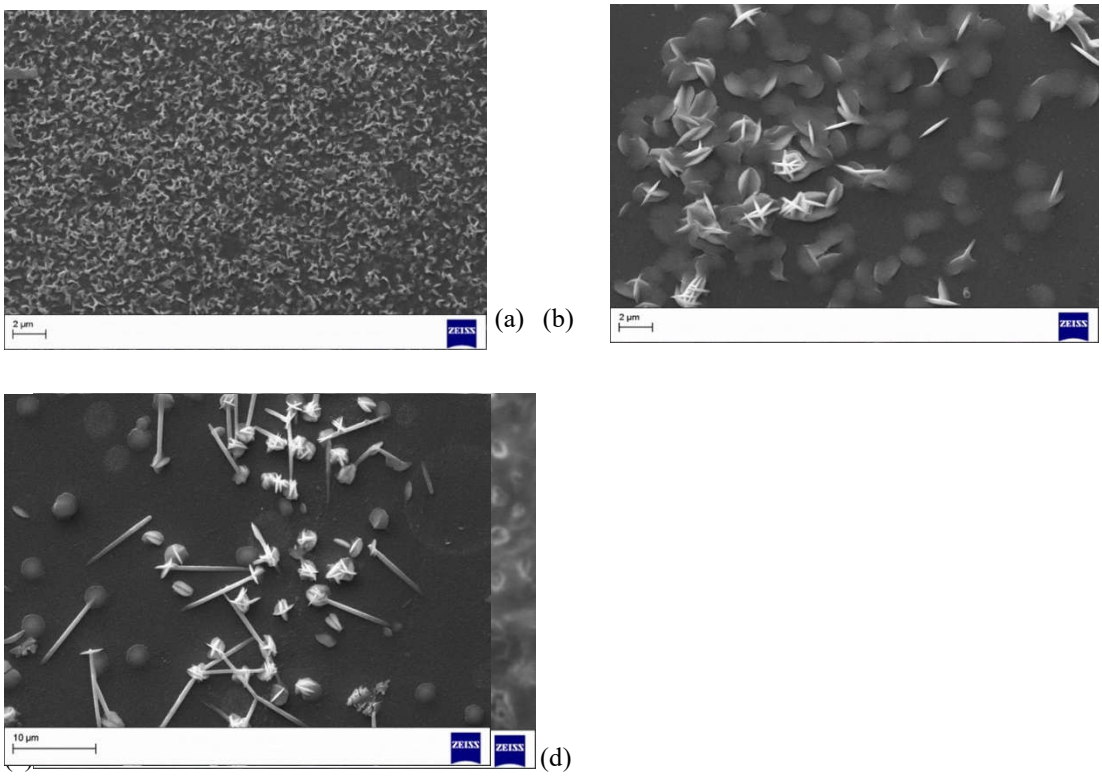

Figure 1.SEM images: (a) WO_3, (b) 5wt% Sn doped (c) 10wt% Sn doped (d) 15wt% Sn doped WO_3 films.

The elemental compositions of the films are determined using EDS. Fig. 2. shows the elemental compositions of the nanostructured WO_3 and Sn-WO_3 films. The nanostructures films contained only W, O and Sn, and no other impurities were observed.

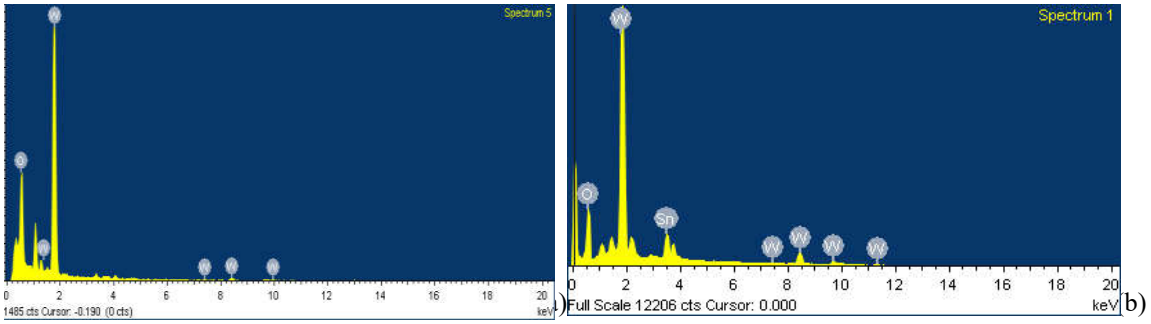

Figure 2. EDS spectra of pure and Sn-WO_3 nanostructure films: (a) WO_3 (b) 10wt% Sn doped WO_3.

3.2 Structural analysis

Figure3 shows the XRD patterns of the WO_3 and Sn-WO_3 films. The WO_3 films exhibited an amorphous nature, and the amorphous nature of the WO_3 films did not change even after dopingwith different Sn concentrations to WO_3, and there were no peaks related to Sn, WO_3, or tin oxide phases. At low temperatures, due to the low energy of tungsten oxide ions reaching the surface of the substrate, and these low energy ions will prevent the crystallization of the WO_3films, consequently, the amorphous phase was obtained [21]. The addition of different Sn concentrationsto WO_3 did not improve the structure of WO_3 films, this may be due to Sn induced stress in the lattice which may continue the amorphous structure of Sn-WO_3 films.

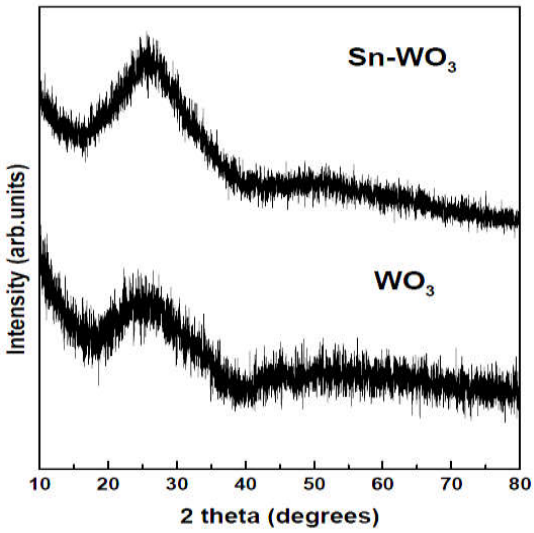

Figure 3.XRD patterns of WO_3 and 10wt% Sn doped WO_3 nanostructure films.

3.3 Optical properties

The optical properties of the films were investigated in the wavelength range of 300 -1200 nm. Fig.4. shows the measured transmittance spectra of nanostructured WO_3 and Sn-WO_3 films at different wt.% of Sn. The average transmittance of the films in the visible region is around 83% for the WO_3films, and it decreased to 79% after adding the Sn to theWO_3. The decrease in transmittance of Sn doped WO_3 films was due to the increase in scattering light caused by the increased of surface roughness of the films and/or tin metal segregate to grain boundaries may cause the decreasing the transmittance. From the transmittance spectra, we observed thatthe absorption edge of the films is shifted towards the longer wavelength region as the wt% of Sn in Sn-WO_3 films increases.

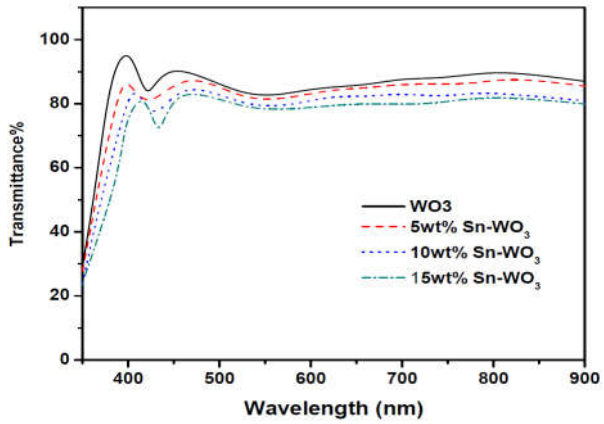

Figure 4.Optical transmittance spectrum of WO_3 and Sn-WO_3 nanostructure films.

The optical band gap (E_g) of the films was evaluated from the extrapolation of the linear portion of the plots of $(\alpha h\nu)^{1/2}$ versus ($h\nu$) (α is the absorption coefficient, $h\nu$ is the photon energy). Fig.5. shows the Tauc plot for nanostructured WO_3 and Sn-WO_3 films. The obtained band gap values are 3.29 eV, 3.25 eV, 3.19 eV and 3.16

eV for WO_3,5wt%Sn-WO_3,10wt%Sn-WO_3,15wt%Sn-WO_3 films, respectively. The larger band gap observed for the deposited thin films can be attributed to their amorphous nature [22].The bandgap of the films decreased gradually from undoped to Sn doped WO_3films. Shankara et al. [20] observed areduction in band gap from 2.62 to 2.46 eV for undoped WO_3 and Sn-doped WO_3 thin films, respectively, due to increase in oxygen vacancies.

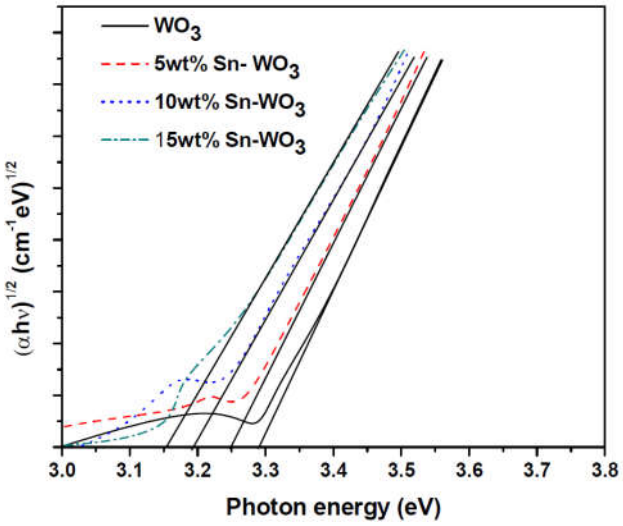

Figure 5.Plot of $(\alpha h\nu)^{1/2}$ vs $(h\nu)$ of WO_3 and Sn-WO_3 nanostructure films.

IV. CONCLUSIONS

Nanostructured $WO_3$and Sn-WO_3 thin films were prepared using the electron beam evaporation method and studied microstructural, structural, chemical, and optical properties. The microstructure of the WO_3 films changed from nanoflakes to rose flakes structure at 5wt% of Sn. On further increasing the dopant concentration to 10wt%, the rose flakes turned into nano nails. The average transmittance of the films in the visible region is around 83% for the WO_3 films, and it decreased to 79% after adding the Sn to the WO_3. The bandgap of the films decreased gradually from undoped to Sn doped WO_3 films.From the present results, we observed that the nanostructure of the WO_3 films is highly influenced by the Sn dopant concentration, and such type of nanostructuredfilms are more suitable for gas sensors applications.

REFERENCES

[1]Manjeet Kumar, Vishwa Bhatt, Akshay Kumar, Ju-Hyung Yun, Nano lily-buds garden like ZnOnanostructures based gas sensor for H_2 Detection, Materials Letters 240 (2019) pp.13–16.https://doi.org/10.1016/j.matlet.2018.12.113
[2] W. Wang, Y. Zhen, J. Zhang, Y. Li, H. Zhong, Z. Jia, Y. Xiong, Q. Xue, Y. Yan, N. S. Alharbi, T. Hayat, SnO_2 nanoparticles-modified 3D-multilayer MoS_2 nanosheets for ammonia gas sensing at room temperature, Sensors Actuators, B Chem 321 (2020) pp.128471. https://doi.org/10.1016/j.snb.2020.128471.
[3] Y. Seekaew, W. Pon-On, C. Wongchoosuk, Ultrahigh selective room-temperature ammonia gas sensor based on tin-titanium dioxide/reduced graphene/carbon nanotube nanocomposites by the solvothermal method, ACS Omega 4 (2019) pp.16916–16924. https://doi.org/10.1021/acsomega.9b02185.
[4] S. Kanaparthi, S.Govind Singh, Highly sensitive and ultra-fast responsive ammonia gas sensor based on 2D ZnO nanoflakes, Mater. Sci. Energy Technol. 3 (2020) pp.91–96.https://doi.org/10.1016/j.mset.2019.10.010.
[5] V. Haridas, A. Sukhananazerin, J. Mary Sneha, B. Pullithadathil, B. Narayanan, α-Fe_2O_3 loaded less-defective graphene sheets as chemiresistive gas sensor for selective sensing of NH3, Appl. Surf. Sci. 517 (2020).pp.146158, https://doi.org/ 10.1016/j.apsusc.2020.146158.
[6] D. Kwak, M. Wang, K.J. Koski, L. Zhang, H. Sokol, R. Maric, Y. Lei, Molybdenum Trioxide (α-MoO_3) Nanoribbons for Ultrasensitive Ammonia (NH_3) Gas Detection: integrated Experimental and Density Functional Theory Simulation Studies, ACS Appl. Mater. Interfaces. 11 (2019) pp.10697–10706.https://doi.org/10.1021/ acsami.8b20502.
[7] D. Kwak, Y. Lei, R. Maric, Ammonia gas sensors: a comprehensive review, Talanta 204 (2019) pp.713–730, https://doi.org/10.1016/j.talanta.2019.06.034.
[8] T.M. Salama, M. Morsy, R.M. Abou Shahba, S.H. Mohamed, M.M. Mohamed, Synthesis of Graphene Oxide Interspersed in Hexagonal WO_3 Nanorods for High- Efficiency Visible-Light Driven Photocatalysis and NH_3 Gas Sensing, Front. Chem. 7 (2019) pp.1–14.https://doi.org/10.3389/fchem.2019.00722
[9] S. Ramkumar, G. Rajarajan, Effect of Fe doping on structural, optical and photocatalytic activity of WO_3 nanostructured thin films, J Mater Sci: Mater Electron, 27 (2016) pp.1847-1853. DOI 10.1007/s10854-015-3963-6
[10] V. Hariharan, S. Radhakrishnan, M. Parthibavarman, R. Dhilipkumar, C. Sekar, Synthesis of polyethylene glycol (PEG) assisted tungsten oxide (WO_3) nanoparticles for L-dopa bio-sensing applications, Talanta 85 (2011) pp.2166–2174. https://doi.org/10.1016/j.talanta.2011.07.063
[11] W. Zhu, J. Liu, S. Yu, Y. Zhou, X. Yan, Ag loaded WO_3 nanoplates for efficient photocatalytic degradation of sulfanilamide and their bactericidal effect under visible light irradiation, J. Hazard Mater. 318 (2016) pp.407–416. https://doi.org/10.1016/j.jhazmat.2016.06.066
[12] M.A. Syed, U. Manzoor, I. Shah, S.H. Bukhari, Antibacterial effects of Tungsten nanoparticles on the Escherichia coli strains isolated from catheterized urinary tract infection (UTI) cases and Staphylococcus aureus, New Microbiologica 33 (2010) pp.329–335.
[13] G. Duan, L. Chen, Z. Jing, P. De Luna, L. Wen, L. Zhang Zhao, et al., Chem. Res. Toxicol. 32 (2019) pp.1357–1366. doi: 10.1021/acs.chemrestox.8b00399.
[14] Adilakshmi Griddaluru, Sivasankar Reddy Akepati,Electron beam evaporated gold doped tungsten oxide nanostructured films for sensor applications, ChemPhysMater 2 (2023) pp.172–179. https://doi.org/10.1016/j.chphma.2022.09.003
[15] Aditya Yadav, Avinash Kumar, Lalit Goswami, Rimjhim Yadav, Anuj Sharma, Govind Gupta, Plasmonic hot electron-induced WO_3 films for a highly responsive visible photodetector, Surfaces and Interfaces42 (2023) pp.103461. https://doi.org/10.1016/j.surfin.2023.103461
[16] Fabien Sanchez, L. Marot, A. Dmitriev, R. Antunes, R. Steiner, E. Meyer, WO_3 work function enhancement induced by filamentous films deposited by resistive heating evaporation technique, J. Alloys and Compounds, 968 (2023)pp.171888. https://doi.org/10.1016/j.jallcom.2023.171888
[17] Vinayak Ganbavle, Shahin Shaikh, Santosh Mohite, Sumayya Inamdar, Amit Bagade, Atish Patil, Keshav Rajpure, Synergistic effects of Pd decoration and substrates on the NO_2 sensing performance of sprayed WO_3 thin films, Chemical Physics Lettes 814 (2023) pp.140327. https://doi.org/10.1016/j.cplett.2023.140327
[18] Qimeng Sun, Songjie Li, Xiaomei Yu, Yanmin Zhang, Tiantian Liu, Jin You Zheng, Amorphous bismuth-doped WO_3 film: Fast-switching time and high-performance proton-based aqueous electrochromic device,Applied Surface Science 641 (2023) pp.158510. https://doi.org/10.1016/j.apsusc.2023.158510
[19] Hongxi Gu, Mengdi Tan, Ting Wang, Jiayi Sun, Juan Du , Rong Ma, Wei Wang, Dengwei Hu, Boosting the electrochromic performance of P-doped WO_3 films *via* electrodeposition for smart window applications, RSC Advances 14(2024) **pp.**10298. https://doi.org/10.1039/d4ra00979g
[20] Shankara S. Kalanur, Structural, Optical, Band Edge and Enhanced Photoelectrochemical Water Splitting Properties of Tin-Doped WO_3, Catalysts, 9 (2019) pp.456. doi:10.3390/catal9050456
[21] Michał Mazura, Damian Wojcieszak, Artur Wiatrowski, Danuta Kaczmarek, Aneta Luba´ nska, Jarosław Domaradzki, Piotr Mazur, Małgorzata Kalisz, Analysis of amorphous tungsten oxide thin films deposited by magnetron sputtering for application in transparent electronics, Applied Surface Science 570 (2021) pp.15115.https://doi.org/10.1016/j.apsusc.2021.151151
[22] Mazur M, Wojcieszak D, Wiatrowski A, Kaczmarek D, Luba_nska A, Domaradzki J, et al. Analysis of amorphous tungsten oxide thin films deposited by magnetron sputteringfor application in transparent electronics. Appl Surf Sci 570 (2021) pp.151151. https://doi.org/10.1016/j.apsusc.2021.151151.